

See discussions, stats, and author profiles for this publication at: <https://www.researchgate.net/publication/6895459>

Gadolinium-Based Mixed-Metal Nitride Clusterfullerenes $Gd_xSc_{3-x}N@C_{80}$ ($x=1, 2$)

ARTICLE in CHEMPHYSCHEM · SEPTEMBER 2006

Impact Factor: 3.42 · DOI: 10.1002/cphc.200600323 · Source: PubMed

CITATIONS

59

READS

30

4 AUTHORS, INCLUDING:



Shangfeng Yang

University of Science and Technology of Ch...

141 PUBLICATIONS 2,847 CITATIONS

SEE PROFILE



Martin Kalbác

Academy of Sciences of the Czech Republic

161 PUBLICATIONS 3,176 CITATIONS

SEE PROFILE



Alexey A Popov

Leibniz Institute for Solid State and Materia...

188 PUBLICATIONS 3,412 CITATIONS

SEE PROFILE

Gadolinium-Based Mixed-Metal Nitride Clusterfullerenes $\text{Gd}_x\text{Sc}_{3-x}\text{N@C}_{80}$ ($x = 1, 2$)**

Shangfeng Yang,^{*,[a]} Martin Kalbac,^[a, b] Alexey Popov,^[c] and Lothar Dunsch^{*,[a]}

The first gadolinium-based mixed-metal nitride clusterfullerenes $\text{Gd}_x\text{Sc}_{3-x}\text{N@C}_{80}$ (I) ($x = 2$; 2, $x = 1$) have been successfully synthesized by the reactive gas atmosphere method and isolated facily by recycling high-performance liquid chromatography (HPLC). The sum yield of 1 and 2 is 30–40 times higher than that of $\text{Gd}_3\text{N@C}_{80}$ (I). Moreover, an enhanced relative yield of 2 over the $\text{Sc}_3\text{N@C}_{80}$ (I) is achieved under the optimized synthesis condi-

tions. According to the UV/Vis/NIR spectroscopic characterization, 1 and 2 are both stable fullerenes with large optical band-gaps while 1 has higher similarity to $\text{Gd}_3\text{N@C}_{80}$ (I) and 2 resembles $\text{Sc}_3\text{N@C}_{80}$ (I). The vibrational structures of 1 and 2 are studied by Fourier-transform infrared (FTIR) spectroscopy as well as density functional theory (DFT) computations. In particular, the structures of the encaged $\text{Gd}_x\text{Sc}_{3-x}\text{N}$ clusters within 1 and 2 are analyzed.

Introduction

Trimetallic nitride endohedral fullerenes (clusterfullerenes) represent a new class of fullerenes with a trimetallic nitride cluster encaged.^[1–2] So far many new clusterfullerenes have been synthesized by tuning the trapped metal atoms and stabilizing a large variety of cage sizes including different isomeric structures.^[1–7]

The Gd-based endohedral fullerenes have great potential in applications as new contrast agents in magnetic resonance imaging (MRI).^[8–10] However, in general the yield of Gd-based endohedral fullerenes in arc synthesis is quite low,^[8–9] discouraging their practical application. With three gadolinium ions encaged, Gd-based nitride clusterfullerenes appear more promising because even higher proton relaxivities can be expected provided that the magnetic moments of the three Gd ions are ferromagnetically coupled. Specifically, among the reported clusterfullerenes, the distinguished uniqueness of $\text{Gd}_3\text{N@C}_{2n}$ clusterfullerene is that Gd_3N represents the largest cluster encaged in fullerene cages to date, while $\text{Gd}_3\text{N@C}_{2n}$ clusterfullerenes have been revealed to exhibit the lowest yield.^[7c, 11] This is largely due to the constraint of the large cluster size of Gd_3N .^[7c] Therefore, it is important to address whether the yield of Gd-based endohedral fullerenes can be improved.

In the clusterfullerene family, fullerenes with two different metals mixed in the encaged nitride (mixed-metal clusterfullerenes) are recognized as the minor members. Few mixed-metal clusterfullerenes have been reported; these include $\text{Er}_x\text{Sc}_{3-x}\text{N@C}_{80}$ ($x = 0–2$),^[1–3, 12, 13] $\text{A}_x\text{Sc}_{3-x}\text{N@C}_{68}$ ($x = 0–2$; $\text{A} = \text{Tm}, \text{Er}, \text{Gd}, \text{Ho}, \text{La}$),^[14] $\text{Lu}_{3-x}\text{A}_x\text{N@C}_{80}$ ($x = 0–2$; $\text{A} = \text{Gd}, \text{Ho}$).^[15] Except for $\text{ErSc}_2\text{N@C}_{80}$ and $\text{Er}_2\text{ScN@C}_{80}$, which have been isolated,^[1, 12, 13] up to now all the mixed-metal nitride clusterfullerenes were only detected by mass spectroscopy (MS) and have not yet been isolated. It has been revealed that, with the variation of the encaged mixed-metal nitride cluster, the symmetry of the carbon cage remains unchanged.^[1, 12, 13] This makes the isolation of the mixed-metal nitride clusterfullerenes quite tedious and

difficult. Even though, a noteworthy feature of the mixed-metal nitride clusterfullerenes is that, based on a rough estimation on the intensity of the negative ion-desorption chemical ionization (NI-DCI) mass-spectral peak, the yield of the mixed-metal nitride clusterfullerenes could be even higher than that of the single metal nitride clusterfullerenes like $\text{Sc}_3\text{N@C}_{80}$.^[3, 14, 15] Such an advantage provides an ideal solution for improving the yield of clusterfullerenes based on those metal atoms such as Gd, whose yield in the form of single-metal nitride clusterfullerenes is quite low. In the case of Gd-based mixed-metal clusterfullerenes with Sc introduced as the second metal atom, a further intriguing question is which structure the Gd-based mixed-metal nitride would take, since the Gd_3N within the $I_h\text{C}_{80}$ cage of $\text{Gd}_3\text{N@C}_{80}$ is pyramidal^[11] while Sc_3N within $\text{Sc}_3\text{N@C}_{80}$ was found to be planar.^[3]

Herein we report the high-yield synthesis of the first Gd-based mixed-metal clusterfullerenes $\text{Gd}_x\text{Sc}_{3-x}\text{N@C}_{80}$ (I) ($x = 1, 2$) by the reactive gas atmosphere method^[1, 2] and their facile isolation by recycling high-performance liquid chromatography (HPLC). The relative yield of $\text{Gd}_x\text{Sc}_{3-x}\text{N@C}_{80}$ (I) ($x = 1, 2$) and the

[a] Dr. S. Yang, Dr. M. Kalbac, Prof. Dr. L. Dunsch
Group of Electrochemistry and Conducting Polymers
Leibniz-Institute for Solid State and Materials Research Dresden
01171 Dresden (Germany)
Fax: (+49) 351-4659-811
E-mail: s.yang@ifw-dresden.de
l.dunsch@ifw-dresden.de

[b] Dr. M. Kalbac
J. Heyrovský Institute of Physical Chemistry
Academy of Sciences of the Czech Republic
Dolejškova 3, 18223 Prague 8 (Czech Republic)

[c] Dr. A. Popov
Department of Chemistry, Moscow State University
Leninskiye Gory, 119992 Moscow (Russia)

[**] Synthesis, Isolation and Spectroscopic Characterization.

Supporting information for this article is available on the WWW under <http://www.chemphyschem.org> or from the author.

optimized synthesis condition are discussed. We also present the first spectroscopic studies of $\text{Gd}_x\text{Sc}_{3-x}\text{N@C}_{80}$ (I) ($x=1, 2$) as well as the analysis of their vibrational structures in combination with DFT theoretical computations.

Results and Discussion

Synthesis of the $\text{Gd}_x\text{Sc}_{3-x}\text{N@C}_{80}$ (I) ($x=1, 2$) Clusterfullerenes

To synthesize the Gd-based mixed-metal nitride clusterfullerenes, Sc is preferred because of the high yield of $\text{Sc}_3\text{N@C}_{80}$ clusterfullerenes, as previously demonstrated.^[1,3,7a] $\text{Gd}_x\text{Sc}_{3-x}\text{N@C}_{80}$ (I, II) ($x=0-3$) clusterfullerenes are synthesized with high yield by the reactive gas atmosphere method.^[1,2] A typical chromatogram of a $\text{Gd}_x\text{Sc}_{3-x}\text{N@C}_{2n}$ fullerene extract mixture obtained under the optimized condition (molar ratio of Gd:Sc = 1:1) is shown in Figure 1, indicating the formation of $\text{Gd}_x\text{Sc}_{3-x}\text{N@C}_{2n}$ clusterfullerenes as the main products in combi-

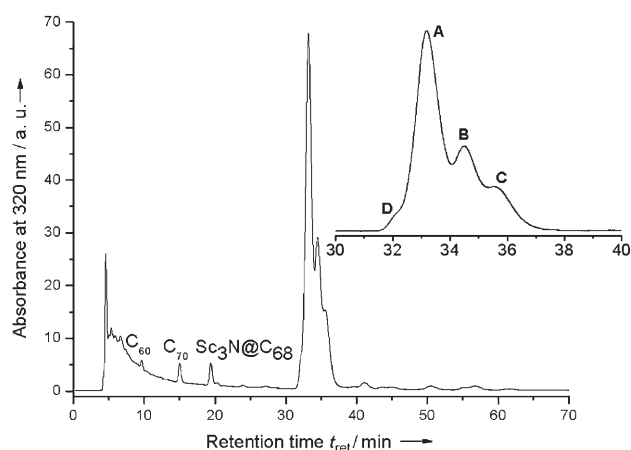


Figure 1. Chromatogram of a $\text{Gd}_x\text{Sc}_{3-x}\text{N@C}_{2n}$ fullerene extract mixture synthesized by the reactive gas atmosphere method (linear combination of two 4.6×250 mm Buckyprep columns; flow rate 1.6 mL min^{-1} ; injection volume $100 \mu\text{L}$; toluene as eluent (mobile phase); 40°C). The inset shows the enlarged chromatographic region of the dominant fractions A–D, which correspond to $\text{Gd}_x\text{Sc}_{3-x}\text{N@C}_{2n}$ (I, II) ($x=0-3$, $2n=78, 80$).

nation with MS analysis. Similar to the case of $\text{Sc}_3\text{N@C}_{2n}$ clusterfullerenes, the abundance of the dominant products ($\text{Gd}_x\text{Sc}_{3-x}\text{N@C}_{80}$ (I, II) ($x=0-3$), fractions A–C, see inset of Figure 1) reaches up to 97% of all the fullerenes, which is significantly higher than that for $\text{Gd}_3\text{N@C}_{2n}$.^[7c] For a typical arc discharge using two graphite rods, the estimated yield of $\text{Gd}_x\text{Sc}_{3-x}\text{N@C}_{80}$ (I) ($x=1, 2$, fraction A) is 30–40 times higher than that of $\text{Gd}_3\text{N@C}_{80}$ (I) by using pure Gd_2O_3 (or Gd) as the starting material (see Supporting Information S1).^[7c]

Isolation of $\text{Gd}_x\text{Sc}_{3-x}\text{N@C}_{80}$ (I) ($x=1, 2$)

A two-step HPLC isolation protocol is established for isolating $\text{Gd}_x\text{Sc}_{3-x}\text{N@C}_{80}$ (I) ($x=1, 2$). Similar to the method used before for isolation of other $\text{M}_3\text{N@C}_{2n}$ ($\text{M}=\text{Sc}, \text{Gd}, \text{Tm}, \text{Dy}$),^[6,7] in the first step HPLC fractions A–D are isolated by using a linear

combination of two Buckyprep columns. The MS analysis indicates that each fraction contains at least two different $\text{Gd}_x\text{Sc}_{3-x}\text{N@C}_{2n}$ ($x=0-3$, $2n=78, 80$) products.^[16] In particular, the most abundant fraction (A) consists of two mixed-metal clusterfullerenes, $\text{Gd}_2\text{ScN@C}_{80}$ (I) (1) and $\text{GdSc}_2\text{N@C}_{80}$ (I) (2), while the main product in fraction B is $\text{Sc}_3\text{N@C}_{80}$ (I) (3). It should be noted that the relative yield of these two fractions is, according to their integrated peak areas, dependent on the molar ratio of Gd:Sc, therefore the optimized condition for the preferable synthesis of the two main mixed-metal clusterfullerenes (1 and 2) has to be determined (see Supporting Information S2). Fraction C is composed of $\text{Gd}_x\text{Sc}_{3-x}\text{N@C}_{80}$ (II) ($x=0-2$) while fraction D primarily consists of $\text{Gd}_x\text{Sc}_{3-x}\text{N@C}_{78}$ ($x=0-2$), which will be reported elsewhere.^[16]

Due to the identity of the cage symmetry in 1 and 2, as revealed below, further isolation of 1 and 2 by an additional step of conventional HPLC using different columns (Buckyprep, Buckyclutcher, and Buckyprep-M) has failed. A successful isolation is thus accomplished by using recycling HPLC, as shown in Figure 2a. Upon recycling with 13 cycles using the Buckyprep-M column, 1 and 2 are completely isolated (see Figure 2b) and laser-desorption time-of-flight (LD-TOF) MS analysis (Figure 3) confirms their composition and high purity ($\geq 99\%$). Likewise, $\text{Sc}_3\text{N@C}_{80}$ (I) (3) is isolated from fraction B, which also contains the minor product $\text{Gd}_2\text{ScN@C}_{80}$ (II).^[16] The relative yield of 1:2:3 is calculated to be about 0.56:2.2:1 based on the integrated areas of the corresponding chromatographic peaks (see Supporting Information S3), indicating an enhanced yield of 2 in comparison with that of $\text{Sc}_3\text{N@C}_{80}$ (I) (3). Compared to the case of $\text{Er}_x\text{Sc}_{3-x}\text{N@C}_{80}$ ($x=0-3$) reported in ref. [3], the relative yield of 2 to 3 is comparable to that of $\text{ErSc}_2\text{N@C}_{80}$ to $\text{Sc}_3\text{N@C}_{80}$. However, the relative yield of 1 to 3 is

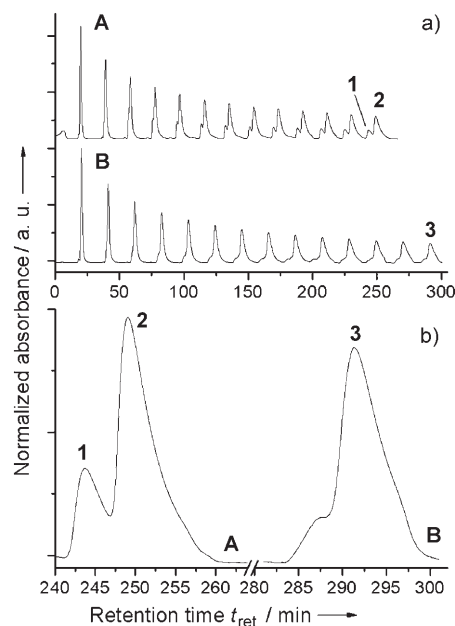


Figure 2. a) Chromatograms of the isolated fractions A and B by recycling HPLC (10×250 mm Buckyprep-M column; flow rate 5.0 mL min^{-1} ; injection volume 5 mL ; toluene as eluent; 25°C). b) Chromatograms of fractions A and B in the final cycle by recycling HPLC based on (a).

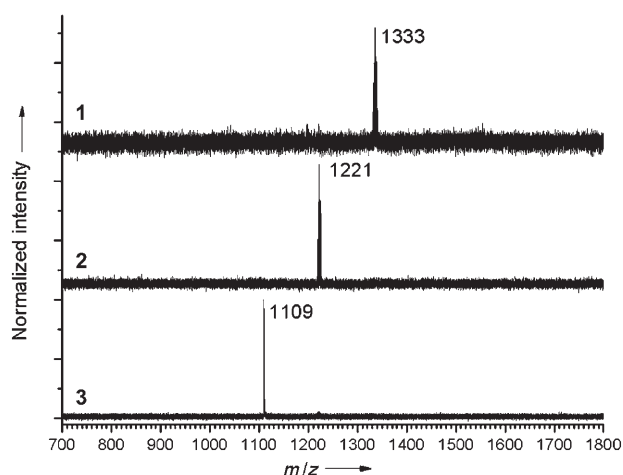


Figure 3. Positive-ion LD-TOF mass spectrum of the isolated $\text{Gd}_x\text{Sc}_{3-x}\text{N}@\text{C}_{80}$ (I). 1: $\text{Gd}_2\text{ScN}@\text{C}_{80}$ (I), $x=2$; 2: $\text{GdSc}_2\text{N}@\text{C}_{80}$ (I), $x=1$; 3: $\text{Sc}_3\text{N}@\text{C}_{80}$ (I), $x=0$.

lower than that of $\text{Er}_2\text{ScN}@\text{C}_{80}$ to $\text{Sc}_3\text{N}@\text{C}_{80}$ [3] obviously due to the larger size of the Gd_2ScN cluster. $\text{Gd}_3\text{N}@\text{C}_{80}$ (I) is detected by MS but has not been isolated in macroscopic amounts because of its negligible yield compared to its analogues 1–3. These results confirm the effect of cluster size on the formation of clusterfullerene for Gd-based clusterfullerenes as revealed in ref. [7c].

Electronic Absorption Spectra of Isolated $\text{Gd}_x\text{Sc}_{3-x}\text{N}@\text{C}_{80}$ (I) ($x=1, 2$)

The UV/Vis/NIR spectra of isolated $\text{Gd}_x\text{Sc}_{3-x}\text{N}@\text{C}_{80}$ (I) ($x=0–3$) dissolved in toluene are shown in Figure 4, indicating the characteristic electronic absorptions which are predominantly due to $\pi-\pi^*$ transitions of the fullerene cage. [6–9] Although the electronic spectra of most endohedral fullerenes are dominated by features of the carbon cage rather than the encapsulated species, the obvious change upon varying the $\text{Gd}_x\text{Sc}_{3-x}\text{N}$ cluster indicates significant perturbation of the C_{80} cage in spite of the

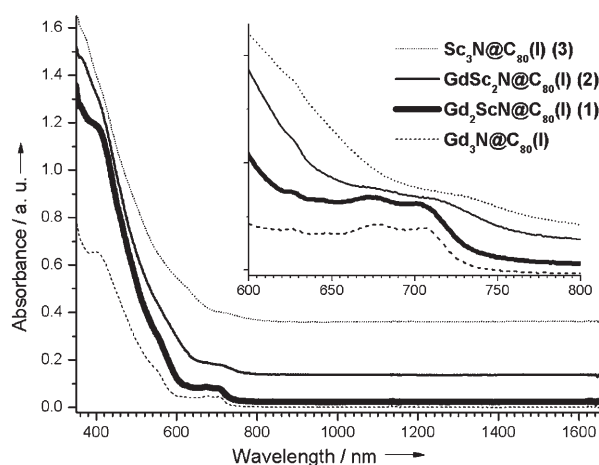


Figure 4. UV/Vis/NIR spectrum of $\text{Gd}_x\text{Sc}_{3-x}\text{N}@\text{C}_{80}$ (I) ($x=0–3$) dissolved in toluene. The inset shows the enlarged spectral range (600–800 nm).

same I_h symmetry. The main difference among the electronic spectra of $\text{Gd}_x\text{Sc}_{3-x}\text{N}@\text{C}_{80}$ (I) ($x=0–3$) is found in the range of 600–700 nm, where $\text{Gd}_x\text{Sc}_{3-x}\text{N}@\text{C}_{80}$ ($x=1,2$) (1 and 2) exhibit intermediate electronic absorption properties in comparison with $\text{Gd}_3\text{N}@\text{C}_{80}$ (I) and $\text{Sc}_3\text{N}@\text{C}_{80}$ (I) (3). [1,7a,c] Although the double peak with absorption maxima at 703 and 672 nm observed in the spectrum of 1 is slightly blue-shifted compared to that of $\text{Gd}_3\text{N}@\text{C}_{80}$ (I) (706 and 676 nm), [7c] the overall absorption feature of $\text{Gd}_3\text{N}@\text{C}_{80}$ (I) is largely preserved by 1. However, in 2 such a feature is dramatically changed to a broad single band with absorption maximum at 712 nm, which is closer to that of $\text{Sc}_3\text{N}@\text{C}_{80}$ (I) (3) even though the absorption maximum is red-shifted to 735 nm (see inset of Figure 4). [1,7a] Compared to the reported electronic absorption spectra of $\text{Er}_x\text{Sc}_{3-x}\text{N}@\text{C}_{80}$ ($x=0–3$), [1] 1 exhibits an almost identical absorption feature to $\text{Er}_2\text{ScN}@\text{C}_{80}$, and the same resemblance is found between 2 and $\text{ErSc}_2\text{N}@\text{C}_{80}$. [1] Nevertheless, for $\text{ErSc}_2\text{N}@\text{C}_{80}$ its absorption maxima (702 and 670 nm) are red-shifted compared to those of $\text{Er}_3\text{N}@\text{C}_{80}$. [1] This is contrary to the shifts observed in 1 compared to $\text{Gd}_3\text{N}@\text{C}_{80}$ (I) as described above. At the higher energy range, the strongest visible absorption peak at 402 nm along with a shoulder peak at 554 nm in the spectrum of $\text{Gd}_3\text{N}@\text{C}_{80}$ (I) follow similar changes, that is, the peak at 412 nm keeps unchanged in the spectrum of 1 while red-shifted in those of 2 and 3. The shoulder peak at 555 nm is almost unchanged in the spectrum of 1 but disappears in those of 2 and 3 (see Figure 4). These results suggest that, in terms of the electronic structure, 1 has a higher similarity to $\text{Gd}_3\text{N}@\text{C}_{80}$ (I), while 2 seems to resemble $\text{Sc}_3\text{N}@\text{C}_{80}$ (I) (3). Since these four $\text{Gd}_x\text{Sc}_{3-x}\text{N}@\text{C}_{80}$ (I) ($x=0–3$) clusterfullerenes have the same cage symmetry (I_h), the similarity/difference of their electronic structure is expected to result from the similarity/difference of the structure of the encaged $\text{Gd}_x\text{Sc}_{3-x}\text{N}$ cluster and its charge transfer to the C_{80} cage.

Regardless of the obvious difference on the characteristic electronic absorptions, the absorption spectral onsets of the four $\text{Gd}_x\text{Sc}_{3-x}\text{N}@\text{C}_{80}$ (I) ($x=0–3$) clusterfullerenes are quite close, which range from about 780 nm in $\text{Gd}_3\text{N}@\text{C}_{80}$ (I) to about 820 nm in 3, suggesting that their optical band gaps are comparable (1.5–1.6 eV). Hence, similar to $\text{Gd}_3\text{N}@\text{C}_{80}$ (I) and $\text{Sc}_3\text{N}@\text{C}_{80}$ (I) (3), 1 and 2 are both stable fullerenes with large optical band-gaps.

Cage-Structure Assignment of $\text{Gd}_x\text{Sc}_{3-x}\text{N}@\text{C}_{80}$ (I) ($x=1, 2$)

Vibrational spectroscopy is a powerful tool for the structural analysis of fullerenes not only due to its high structural sensitivity but also because of its higher time resolution compared to NMR spectroscopy. [1,2,5–7] Figure 5 compares the FTIR spectra of $\text{Gd}_x\text{Sc}_{3-x}\text{N}@\text{C}_{80}$ (I) ($x=0–3$), showing a small number of lines for each fullerene. As we have established in our previous work, [6b–d,7a–d,17] the region of 1100–1600 cm^{-1} is featured by the tangential C_{80} modes and the band around 500 cm^{-1} is correlated with the radial cage mode. These two characteristic bands of 1 and 2 are almost identical for $\text{Gd}_3\text{N}@\text{C}_{80}$ (I), $\text{Sc}_3\text{N}@\text{C}_{80}$ (I) (3) and other known $\text{M}_3\text{N}@\text{C}_{80}$ (I) ($\text{M}=\text{Sc}, \text{Tb}, \text{Ho}, \text{Y}, \text{Er}, \text{Tm}, \text{Gd}$) with an icosahedral C_{80} cage. [1,2,6c,7a–c,17] Therefore,

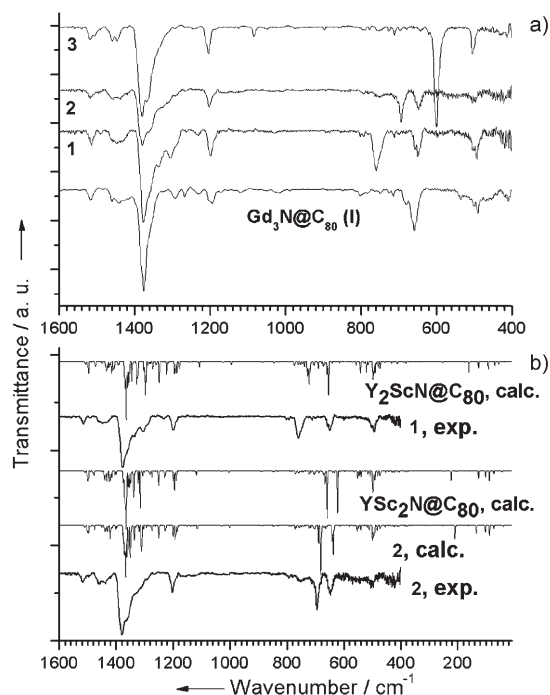


Figure 5. a) FTIR spectra of $\text{Gd}_x\text{Sc}_{3-x}\text{N}@\text{C}_{80}$ (I) ($x=0-3$). For clarity, the spectra of 1–3 are shifted upwards. b) Experimental (exp.) FTIR spectra of 1 and 2 compared to calculated (calc.) spectra of 2, $\text{YSc}_2\text{N}@\text{C}_{80}$ and $\text{Y}_2\text{ScN}@\text{C}_{80}$ based on the I_h C_{80} cage. For Y-containing molecules vibrational spectra are computed using Gd atomic mass for Y atoms.

the same carbon cage, that is C_{80-7} with I_h symmetry,^[1,2,6c,7a-c,17,18] is assigned to 1 and 2 due to these similarities.

On the other hand, the most intense low-energy IR lines in the region of $600-800\text{ cm}^{-1}$, which are assigned to the antisymmetric M–N stretching vibration because of the strong metal dependence,^[1,2,6c,7a-c,17] exhibit a dramatic difference for $\text{Gd}_x\text{Sc}_{3-x}\text{N}@\text{C}_{80}$ (I) ($x=0-3$) (Figure 5a). In particular, while only one line is observed in $\text{Gd}_3\text{N}@\text{C}_{80}$ (I) (657 cm^{-1})^[7c] and $\text{Sc}_3\text{N}@\text{C}_{80}$

(I) (3) (599 cm^{-1}),^[7a] in 1 and 2 it is splitted into two components (650 and 760 cm^{-1} for 1, 647 and 694 cm^{-1} for 2) with comparable intensities. It should be noted that the Sc_3N cluster in $\text{Sc}_3\text{N}@\text{C}_{68,78,80}$ has at least threefold symmetry, and thus the Sc–N antisymmetric vibration is twofold degenerated. The same is true for other $\text{M}_3\text{N}@\text{C}_{80}$ clusterfullerenes ($\text{M}=\text{Y}$, Gd–Lu),^[1,2,6c,7a-c,17] where M_3N adopts C_3 symmetry. Substitution of one atom in M_3N cluster by another metal reduces the symmetry of the cluster and hence lifts the degeneracy of the antisymmetric M–N mode.

Cluster Structures of $\text{Gd}_x\text{Sc}_{3-x}\text{N}@\text{C}_{80}$ (I) ($x=1, 2$) Studied by FTIR Spectroscopy and DFT

To understand the behavior of the splitting of the M–N vibration bands as well as the structure of the mixed-metal nitride cluster, we performed a series of DFT calculations of the geometry parameters and vibrational spectra in clusterfullerenes.^[6d,7d] The atomic Gd has a half-filled f -shell with seven unpaired electrons, and thus the Gd-containing molecules have high multiplicities (8 for $\text{GdSc}_2\text{N}@\text{C}_{80}$, 15 for $\text{Gd}_2\text{ScN}@\text{C}_{80}$). This causes serious problems with the convergence of self-consistent field (SCF) equations particularly for $\text{Gd}_2\text{ScN}@\text{C}_{80}$. Therefore the calculations were successful only for $\text{GdSc}_2\text{N}@\text{C}_{80}$ (I) (2). To get an approximation for the vibrational spectra of $\text{Gd}_2\text{ScN}@\text{C}_{80}$ (I) (1) we used Y- and Lu-based clusterfullerenes for the calculations as these elements do not have partially filled f -shells.

Table 1 summarizes the DFT-optimized metal-nitrogen bond lengths (d), computed M–N stretching frequencies (ν , DFT) and effective force constants (k) evaluated by using equations S7–S9 (see Supporting Information S4). Figure 5b shows the experimental (exp.) and calculated (calc.) FTIR spectra of 1 and 2 in comparison with the calculated (calc.) spectra of $\text{GdSc}_2\text{N}@\text{C}_{80}$, $\text{YSc}_2\text{N}@\text{C}_{80}$ and $\text{Y}_2\text{ScN}@\text{C}_{80}$ which have the same I_h C_{80} cages. The DFT-computed spectrum of 2 shows good agreement with the measured data. Unlike $\text{LuSc}_2\text{N}@\text{C}_{80}$ (not

Table 1. Computed Sc–N and M–N bond length (d), antisymmetric stretching vibrational frequencies (ν , DFT) and effective force constants (k) (estimated from equations S7–S9 in Supporting Information) as well as experimental vibrational frequencies (ν , exp.) in $\text{M}_x\text{Sc}_{3-x}\text{N}@\text{C}_{80}$ ($x=0-3$) (C_{80-I_h}) clusterfullerenes.

x		$d_{\text{Sc-N}}$ [Å]	$\nu_{\text{Sc-N exp.}}$ [cm^{-1}]	$\nu_{\text{Sc-N DFT}}$ [cm^{-1}]	$k_{\text{Sc-N DFT}}$ [aJ Å^{-2}]	$d_{\text{M-N}}$ [Å]	$\nu_{\text{M-N exp.}}$ [cm^{-1}]	$\nu_{\text{M-N DFT}}$ [cm^{-1}]	$k_{\text{M-N DFT}}$ [aJ Å^{-2}]
0	$\text{Sc}_3\text{N}@\text{C}_{80}$ (3)	2.034	599	579	0.909				
	$\text{Sc}_3\text{N}@\text{C}_{78}$ ^[7d]	2.012	622, 629	608	1.003				
	$\text{Sc}_3\text{N}@\text{C}_{68}$ ^[6d]	1.993	661	638	1.104				
1	$\text{LuSc}_2\text{N}@\text{C}_{80}$	1.988, 1.993		645	1.128	2.147		646	1.128
	$\text{YSc}_2\text{N}@\text{C}_{80}$	1.979, 1.985		658	1.174	2.160		623	0.993
	$\text{GdSc}_2\text{N}@\text{C}_{80}$ (2)	1.965, 1.972	694	682	1.262	2.194	647	638	1.023
2	$\text{Lu}_2\text{ScN}@\text{C}_{80}$	1.945		715, 720, 725	1.469	2.104, 2.107		686	1.276
	$\text{Y}_2\text{ScN}@\text{C}_{80}$	1.932		719, 723	1.505	2.111, 2.107		663, 664	1.195
	$\text{Gd}_2\text{ScN}@\text{C}_{80}$ (1)	1.886 ^[a]	759				649, 656		
3	$\text{Lu}_3\text{N}@\text{C}_{80}$					2.062		750	1.526
	$\text{Y}_3\text{N}@\text{C}_{80}$					2.060	712, 724	733	1.457
	$\text{Gd}_3\text{N}@\text{C}_{80}$						657		

[a] This value is estimated from the correlation of experimental $k_{\text{Sc-N}}$ and DFT optimized $d_{\text{Sc-N}}$ (see Supporting Information S5).

shown), the computed spectrum of $\text{YSc}_2\text{N@C}_{80}$ appears to be rather close to the data for **2** (see Figure 5b), although the predicted M–N frequencies are somewhat lower (see Table 1). If we assume that this similarity is also preserved for $\text{Gd}_2\text{ScN@C}_{80}$, the calculated spectrum of $\text{Y}_2\text{ScN@C}_{80}$ can be used for the assignment of the vibrational features of **1**.

The general trend found for all computed $\text{M}_x\text{Sc}_{3-x}\text{N@C}_{80}$ ($\text{M} = \text{Lu}, \text{Y}, \text{Gd}$) clusterfullerenes is the synchronous shortening of Sc–N and M–N bonds with increasing x (see Table 1). The N atom, which is located on the C_3 axis in $\text{Sc}_3\text{N@C}_{80}$ (see Figure 6), is displaced towards the Sc atoms in the case of $\text{MSc}_2\text{N@C}_{80}$ and $\text{M}_2\text{ScN@C}_{80}$. This indicates that M_3N clusters suffer the inherent strain due to the larger size of M atoms and the shorter M–N bonds. For $\text{MSc}_2\text{N@C}_{80}$ and $\text{M}_2\text{ScN@C}_{80}$, the strain can be partially transferred to the Sc–N bond. This leads to the elongation of the M–N bond compared to

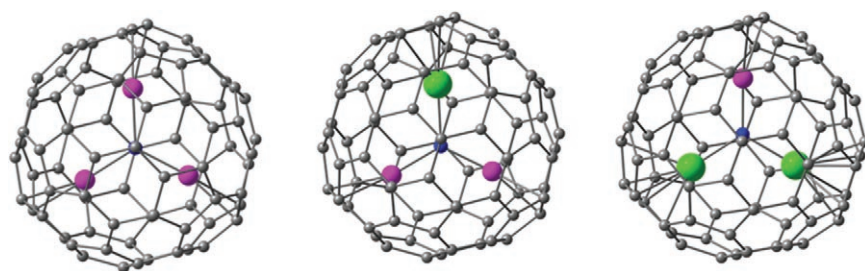


Figure 6. DFT-optimized $\text{Sc}_3\text{N@C}_{80}$ (left), $\text{YSc}_2\text{N@C}_{80}$ (middle) and $\text{Y}_2\text{ScN@C}_{80}$ (right) viewed along C_3 axis of the I_h C_{80} cage. The Sc, Y, and N atoms are drawn in violet, green, and blue, respectively. The latter two are also proposed to be the structures of **2** and **1**, respectively.

$\text{M}_3\text{N@C}_{80}$ and the shortening of the Sc–N bond compared to $\text{Sc}_3\text{N@C}_{80}$. For $\text{M}_2\text{ScN@C}_{80}$, the strain is transferred to one Sc–N bond only, while if the second M atom is further replaced, the steric hindrance is suffered by two Sc–N bonds. Therefore, $d_{\text{Sc–N}}$ should decrease in the sequence $\text{Sc}_3\text{N@C}_{80} \rightarrow \text{MSc}_2\text{N@C}_{80} \rightarrow \text{M}_2\text{ScN@C}_{80}$. Accordingly $\nu_{\text{Sc–N}}$ should increase in the same sequence. This is confirmed by the experimental spectra as the $\nu_{\text{Sc–N}}$ vibrations are found at 599, 694 and 759 cm^{-1} for $\text{Sc}_3\text{N@C}_{80}$ (**3**), **2**, and **1** respectively. A similar trend is reported for $\text{Er}_x\text{Sc}_{3-x}\text{N@C}_{80}$ (**I**) clusterfullerenes, for which the $\nu_{\text{Sc–N}}$ vibrations are at 667 and 725 cm^{-1} for $\text{ErSc}_2\text{N@C}_{80}$ and $\text{Er}_2\text{ScN@C}_{80}$, respectively.^[1]

Likewise, the M–N bond lengths ($d_{\text{M–N}}$) decrease and thus $\nu_{\text{M–N}}$ increases in the sequence $\text{MSc}_2\text{N@C}_{80} \rightarrow \text{M}_2\text{ScN@C}_{80} \rightarrow \text{M}_3\text{N@C}_{80}$ as the cluster becomes increasingly strained. Experimental values confirm this tendency. For instance, the Er–N stretching frequencies ($\nu_{\text{Er–N}}$) in $\text{Er}_x\text{Sc}_{3-x}\text{N@C}_{80}$ are found at 647, 661 and $704/713\text{ cm}^{-1}$ for $x=1, 2$, and 3, respectively. The change in $d_{\text{Sc–N}}$ and $\nu_{\text{Sc–N}}$ observed for $\text{Gd}_x\text{Sc}_{3-x}\text{N@C}_{80}$ indicates that the strain for Gd-based clusterfullerenes is probably the highest among the studied molecules. This is also in agreement with the large atomic radius of Gd. With this respect, it might be expected that the changes in $\nu_{\text{Gd–N}}$ should be the most pronounced and $\nu_{\text{Gd–N}}$ should also be the highest among all other $\text{M}_3\text{N@C}_{80}$. Surprisingly, the Gd–N stretching frequencies ($\nu_{\text{Gd–N}}$) are found at 647, 649 and 657 cm^{-1} in $\text{GdSc}_2\text{N@C}_{80}$,

$\text{Gd}_2\text{ScN@C}_{80}$ and $\text{Gd}_3\text{N@C}_{80}$, respectively; that is, the trend is substantially less pronounced than in Er-based clusterfullerenes. Moreover, $\nu_{\text{Gd–N}}$ in $\text{Gd}_3\text{N@C}_{80}$ is significantly smaller than that in $\text{Y}_3\text{N@C}_{80}$ ($712/724\text{ cm}^{-1}$)^[5] and all other $\text{M}_3\text{N@C}_{80}$ clusterfullerenes studied to date ($700\text{--}720\text{ cm}^{-1}$ for Dy, Tm, Er, Ho; $669/689\text{ cm}^{-1}$ for Tb).^[1,2,6c,7a–c] This apparent disagreement is partially understood by considering that the Gd_3N unit in $\text{Gd}_3\text{N@C}_{80}$ is pyramidal with the N atom displaced about 0.5 \AA above the plane of Gd atoms, as shown by X-ray crystallographic data.^[11] This suggests that the strain in Gd_3N is so strong that N atoms are pushed out of the Gd_3 plane. If the C_3 symmetry found for other $\text{M}_3\text{N@C}_{80}$ is still preserved in $\text{Gd}_3\text{N@C}_{80}$, the antisymmetric Gd–N stretching vibration, which belongs to E type in C_3 symmetry group, corresponds to the displacement of the N atom in the plane perpendicular to C_3 axis. Thus, the effective force constant (k), which governs the

frequency of this mode, is reduced by the factor $\cos^2\beta$, where β is the angle between the Gd–N bond and the Gd_3 plane. Note that a recent X-ray crystallography study of $\text{Dy}_3\text{N@C}_{80}$ (**I**) revealed that Dy_3N is planar.^[19] Thus, a planar structure of the cluster is proposed for all $\text{M}_3\text{N@C}_{80}$ with M smaller than Dy, including all $\text{Er}_x\text{Sc}_{3-x}\text{N}$ clusterfullerenes.

Based on the analysis given above, it appears that the increase of x in $\text{Gd}_x\text{Sc}_{3-x}\text{N@C}_{80}$ ($x=0\text{--}3$) clusterfullerenes results in a shortening of the Gd–N bond (i.e. increase of the force constant). At the same time a pyramidalization of the cluster occurs (i.e. reduction of the effective force constant). Accordingly, these two factors partially compensate each other, leaving the frequency of the Gd–N mode almost unchanged. Similar to $\text{Sc}_3\text{N@C}_{80}$ (**3**), the DFT calculation predicts that the GdSc_2N unit in $\text{GdSc}_2\text{N@C}_{80}$ (**2**) is planar. For $\text{Gd}_2\text{ScN@C}_{80}$ (**1**), it is then reasonable to assume that the Gd_2ScN unit is pyramidal instead. More experimental details are required to understand these results fully.

Conclusions

We report the first high-yield synthesis of the Gd-based mixed-metal nitride clusterfullerenes, $\text{Gd}_x\text{Sc}_{3-x}\text{N@C}_{80}$ (**I**) ($x=1, 2$), by the reactive gas atmosphere method and their facile isolation by recycling HPLC. The relative yield of the two $\text{Gd}_x\text{Sc}_{3-x}\text{N@C}_{80}$ (**I**) (**1**, $x=2$; **2**, $x=1$) compared to that of $\text{Sc}_3\text{N@C}_{80}$ (**I**) (**3**) under the optimized synthesis condition is estimated, indicating an enhanced yield of **2** in comparison with **3**. The UV/Vis/NIR spectroscopic characterization indicates that **1** and **2** are both stable fullerenes with large optical band-gaps while **1** has higher similarity to $\text{Gd}_3\text{N@C}_{80}$ (**I**) and **2** resembles **3**. The vibrational structures of **1** and **2** were studied by FTIR spectroscopy as well as DFT computations. The good agreement between the measured FTIR spectrum of **2** and its DFT-computed spec-

trum confirms that the GdSc_2N unit in $\text{GdSc}_2\text{N@C}_{80}$ (**2**) is planar. However, based on the detailed analysis of the bond lengths and vibrational frequencies of the antisymmetric stretching modes of both Gd–N and Sc–N bonds, it is expected that the Gd_2ScN unit in $\text{Gd}_2\text{ScN@C}_{80}$ (**1**) is pyramidal. The final elucidation of the cluster structure of **1** is currently underway and will be established with X-ray crystallography.

Experimental Section

General procedures for the production of $\text{Gd}_x\text{Sc}_{3-x}\text{N@C}_{80}$ (**1**) ($x=1, 2$) by a modified Krätschmer–Huffman direct current (dc)-arc discharging method with the addition of NH_3 (20 mbar) have been described elsewhere.^[1,2,4–7] Briefly, a mixture of Gd_2O_3 and Sc_2O_3 (99.9%, MaTeck GmbH, Germany) and graphite powder was used with various Gd:Sc molar ratios [from 10:1 to 1:2 (typically 1:1)] to study the effect of the mixing ratio on the yield of the mixed-metal nitride clusterfullerenes (molar ratio of Gd:C is fixed at 1:15). After dc-arc discharging, the soot was pre-extracted by acetone and further Soxhlet-extracted by CS_2 for 20 h. Fullerene isolation was performed by two-step HPLC. In the first step, running in a Hewlett Packard instrument (series 1050), a linear combination of two analytical 4.6×250 mm Buckyprep columns (Nacalai Tesque, Japan) was applied with toluene as the eluent. The second-step isolation was performed by recycling HPLC (Sunchrom, Germany) using a semi-preparative Buckyprep-M column (Nacalai Tesque, Japan) with toluene as the eluent. An UV detector set to 320 nm was used for fullerene detection for both steps. The purity of the isolated products was checked by LD-TOF MS analysis running in both positive- and negative-ion modes (Biflex III, Bruker, Germany). Sample preparation and experimental details for UV/Vis/NIR and FTIR spectroscopic measurements have been described previously.^[5–7]

DFT computations were performed with the use of PRIRODA package^[20] and PBE (Perdew–Burke–Ernzerhof) density functional.^[21] TZ2P-quality basis set implemented in the code was used for the C and N atoms, while the basis sets for the Sc, Y, Gd and Lu atoms, comprised of SBK-type^[22] effective-core potential and TZ2P valence part.

Acknowledgements

We cordially thank Ms. K. Leger, Mr. F. Ziegls, and Mrs. H. Zöller for technical assistance and Dr. M. Krause for valuable discussions. S.Y. and M.K. thank the Alexander von Humboldt (AvH) Foundation for financial support. Computer time at the Research Computing Center of the Moscow State University for A.P. is gratefully acknowledged.

Keywords: cluster compounds • density functional calculations • fullerenes • structure elucidation • vibrational spectroscopy

- [1] L. Dunsch, M. Krause, J. Noack, P. Georgi, *J. Phys. Chem. Solids* **2004**, *65*, 309–315.
- [2] L. Dunsch, S. Yang, unpublished results.
- [3] S. Stevenson, G. Rice, T. Glass, K. Harich, F. Cromer, M. R. Jordan, J. Craft, E. Hajdu, R. Bible, M. M. Olmstead, K. Maitra, A. J. Fisher, A. L. Balch, H. C. Dorn, *Nature* **1999**, *401*, 55–57.
- [4] L. Dunsch, P. Georgi, M. Krause, C. R. Wang, *Synth. Met.* **2003**, *135*, 761–762.
- [5] L. Dunsch, P. Georgi, F. Ziegls, H. Zöller, German Patent DE 10301722A1, **2003**.
- [6] a) S. F. Yang, L. Dunsch, *J. Phys. Chem. B* **2005**, *109*, 12320–12328; b) S. F. Yang, L. Dunsch, *Angew. Chem.* **2006**, *118*, 1321–1324; *Angew. Chem. Int. Ed.* **2006**, *45*, 1299–1302; c) S. F. Yang, L. Dunsch, *Chem. Eur. J.* **2006**, *12*, 413–419; d) S. F. Yang, M. Kalbac, A. Popov, L. Dunsch, *Chem. Eur. J.* **2006**, DOI: 10.1002/chem.2006261.
- [7] a) M. Krause, L. Dunsch, *ChemPhysChem* **2004**, *5*, 1445–1449; b) M. Krause, J. Wong, L. Dunsch, *Chem. Eur. J.* **2005**, *11*, 706–711; c) M. Krause, L. Dunsch, *Angew. Chem.* **2005**, *117*, 1581–1584; *Angew. Chem. Int. Ed.* **2005**, *44*, 1557–1560; d) M. Krause, A. Popov, L. Dunsch, *ChemPhysChem* **2006**, DOI: 10.1002/cphc.200600139.
- [8] H. Shinohara, *Rep. Prog. Phys.* **2000**, *63*, 843–892.
- [9] *Endofullerenes: A New Family of Carbon Cluster* (Eds.: T. Akasaka, S. Nagase), Kluwer, Dordrecht, **2002**.
- [10] L. J. Wilson, D. W. Cagle, T. P. Thrash, S. J. Kennel, S. Mirzadeh, J. M. Alford, G. J. Ehrhardt, *Coord. Chem. Rev.* **1999**, *192*, 199–207.
- [11] S. Stevensen, J. P. Phillips, J. E. Reid, M. M. Olmstead, S. P. Rath, A. L. Balch, *Chem. Commun.* **2004**, 2814–2815.
- [12] M. M. Olmstead, A. de Bettencourt-Dias, J. C. Duchamp, S. Stevenson, H. C. Dorn, A. L. Balch, *J. Am. Chem. Soc.* **2000**, *122*, 12220–12226.
- [13] a) R. M. Macfarlane, D. S. Bethune, S. Stevenson, H. C. Dorn, *Chem. Phys. Lett.* **2001**, *343*, 229–234; b) I. N. Ioffe, A. S. Ilevlev, O. V. Boltalina, L. N. Sidorov, H. C. Dorn, S. Stevenson, G. Rice, *Int. J. Mass Spectrom.* **2002**, *213*, 183–189.
- [14] S. Stevenson, P. W. Fowler, T. Heine, J. C. Duchamp, G. Rice, T. Glass, K. Harich, E. Hajdu, R. Bible, H. C. Dorn, *Nature* **2000**, *408*, 427–428.
- [15] E. B. Iezzi, J. C. Duchamp, K. R. Fletcher, T. E. Glass, H. C. Dorn, *Nano Lett.* **2002**, *2*, 1187–1190.
- [16] S. F. Yang, M. Kalbac, A. Popov, L. Dunsch, unpublished results.
- [17] M. Krause, H. Kuzmany, P. Georgi, L. Dunsch, K. Vietze, G. Seifert, *J. Chem. Phys.* **2001**, *115*, 6596–6605.
- [18] P. W. Fowler, D. E. Manolopoulos, *An Atlas of Fullerenes*, Clarendon, Oxford, **1995**.
- [19] S. F. Yang, L. Dunsch, S. I. Troyanov, unpublished results.
- [20] D. N. Laikov, *Chem. Phys. Lett.* **1997**, *281*, 151–156.
- [21] J. P. Perdew, K. Burke, M. Ernzerhof, *Phys. Rev. Lett.* **1996**, *77*, 3865–3868.
- [22] W. J. Stevens, M. Krauss, H. Basch, P. G. Jasien, *Can. J. Chem.* **1992**, *70*, 612–630.

Received: May 23, 2006

Published online on August 7, 2006